Article

Synthesis of polyacene by using a metal–organic framework

Check for updates

Takashi Kitao [1,2,9], Takumi Miura[1,9], Ryo Nakayama [3,4], Yusuke Tsutsui [2,5], Yee Seng Chan[6], Hironobu Hayashi[2,6,7], Hiroko Yamada [6,8], Shu Seki [5], Taro Hitosugi [3,4] & Takashi Uemura [1] ✉

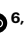The acene series, an important class of linearly polycyclic aromatic hydrocarbons, are of interest owing to their unique physicochemical features. With an increase in the number of fused benzene rings, acenes display an evolution of electronic structure and properties. Thus, efforts have been devoted to the synthesis of longer acenes, with dodecacene being the longest acene (12 fused benzene rings) reported to date. However, the formation of polymeric acenes with numerous benzene rings, namely polyacene, has yet to be realized. Herein, we present a methodology for the synthesis of polyacene mediated by a metal–organic framework. Nanoconfined synthesis of precursor polymers in the channels of the metal–organic framework and the subsequent dehydro-aromatization reaction produced polyacene that was overwhelmingly longer than the previously reported acenes. The scalable synthesis of polyacene allowed us to unveil the stability and electronic properties of polyacene, paving the way for their widespread applications in optoelectronic and magnetic devices.

Since the synthesis of pentacene was reported in 1912 (ref. 1), extension of linearly fused benzene rings has attracted research attention because of curiosity around the nature of aromatic molecules and their applications in optoelectronic nanodevices and biological imaging[2–9]. However, the synthesis of acenes longer than hexacene remains formidably challenging because of their low solubility and chemical instability, as explained by Clar's sextet theory[10]. More specifically, this theory explains how increases in the number of non-sextet rings along the acene series endows molecules with an unstable biradical character in their ground state[11]. Much effort has gone into the synthesis of acenes, and their length has gradually increased (one benzene ring at a time) for many decades. Functionalization with solubilizing and stabilizing substituents has allowed for the preparation of acenes of up to nine fused rings using solution synthesis methods[12]. The on-surface reaction has also emerged as a promising method to afford unsubstituted acenes

under high-vacuum conditions[13,14]. This methodology has enabled the synthesis of the longest acene yet, one with 12 benzene rings[15]. However, despite these efforts, polymeric acenes consisting of numerous fused benzene rings, namely polyacene, have not been synthesized.

Using regular nanopores for ship-in-a-bottle synthesis has many advantages, including highly specific reactions in the pores and imposing nanoconfinement effects on reaction selectivity and kinetics[16–25]. Recently, metal–organic frameworks (MOFs), which comprise metal ions and organic ligands, have attracted much attention due to their applications in fields such as gas storage, separation, catalysts and drug delivery[26–30]. One of the characteristic features of MOFs is their structural diversity; their pore size and shape are controllable at the molecular level, providing an ideal compartment for encapsulating a variety of guest species and controlling their assembly structures[31,32]. The resulting guest molecules can be easily recovered by dissolution

[1]Department of Applied Chemistry, Graduate School of Engineering, The University of Tokyo, Tokyo, Japan. [2]JST-PRESTO, Kawaguchi, Japan. [3]School of Materials and Chemical Technology, Tokyo Institute of Technology, Tokyo, Japan. [4]Department of Chemistry, The University of Tokyo, Tokyo, Japan. [5]Department of Molecular Engineering, Graduate School of Engineering, Kyoto University, Kyoto, Japan. [6]Division of Materials Science, Nara Institute of Science and Technology (NAIST), Ikoma, Japan. [7]Present address: Research Center for Advanced Measurement and Characterization, National Institute for Materials Science (NIMS), Tsukuba, Japan. [8]Present address: Institute for Chemical Research, Kyoto University, Kyoto, Japan. [9]These authors contributed equally: Takashi Kitao, Takumi Miura. ✉e-mail: uemurat@g.ecc.u-tokyo.ac.jp
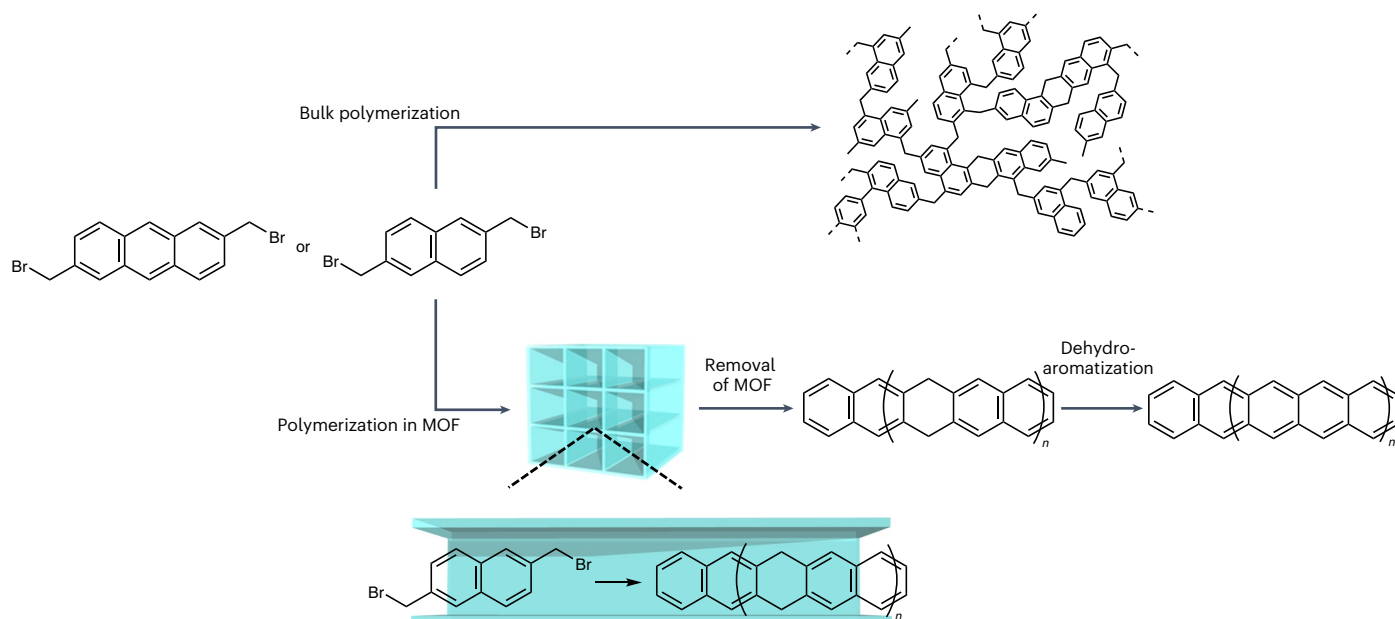
Fig. 1 | Schematic of polyacene synthesis using an MOF. An MOF with 1-D nanochannels is used as a reaction template, in which monomers can be aligned along the channel direction. Selective coupling reaction of the monomers at the 3- and 7-position leads to the formation of precursor polymers. The subsequent dehydro-aromatization reaction of the precursor polymers affords polyacene in the bulk scale.

of the host frameworks, affording well-defined nanomaterials with accurately controlled structures.

Here, we report the synthesis of polyacene by using a methodology, distinct from conventional methods, grounded on organic and/or surface chemistry. The proposed strategy involves two steps: controlled synthesis of precursor polymers within an MOF and subsequent conversion into polyacene (Fig. 1). The spatial constraints of the MOF allowed for the highly regulated polycoupling reaction of aromatic monomers within the one-dimensional (1-D) nanochannels, providing linearly extended polymeric precursors. Subsequently, the dehydro-aromatization reaction of the precursors provided the bulk quantity of polyacene without any peripheries, which was inaccessible using conventional methods.

Results and discussion

Hydroacenes, the partially saturated acenes, can be used as precursors of acenes via dehydro-aromatization[33]. Therefore, we envisioned that polymeric hydroacenes could serve as a precursor for the generation of polyacene. For this purpose, 2,6-bis(bromomethyl)naphthalene (BBMN) and 2,6-bis(bromomethyl)anthracene (BBMA) could be used as monomers if the selective coupling reaction would proceed at the 3- and 7-position. However, targeted precursor polymers were not obtained in the bulk reaction owing to the higher reactivity at zigzag positions than at the 3- and 7-position (Fig. 1 and Supplementary Fig. 1). Thermal treatment of the neat BBMN resulted in the formation of branched and graphitic structures (Supplementary Fig. 2).

To initiate the site-selective polycoupling reaction, an MOF with 1-D nanochannels was used as a host in which the monomers could be aligned along the channel direction. We used $[ZrO(L)]_n$ (where L is the dicarboxylate ligand), with 1-D nanochannels along the c-axis, as the host because its pore size can be tuned at the molecular level by changing the dicarboxylate ligand[34]. Additionally, $[ZrO(L)]_n$ has high thermal stability because of the strong coordination bond and high coordination number of the zirconium nodes. On the basis of the molecular dimensions of BBMN (4.9×8.5 Å^2) and BBMA (4.9×11.2 Å^2), $[ZrO(4,4\text{-biphenyldicarboxylate})]_n$ (**1**; pore size = 6.9×6.9 Å^2) was used as a host for the selective propagation of linear polymer chains (Supplementary Fig. 3a). Molecular dynamics (MD) simulations revealed that the accommodated monomers were densely assembled in an

end-to-end fashion due to the geometrical constraint and host–guest interactions (Supplementary Fig. 3b,c), which would facilitate the regulated reactions at the 3- and 7-position of the monomers.

Polymerization of the monomers in the nanochannels of **1** was performed as follows. First, the monomers were introduced into the pores of **1** by sublimation to obtain the host–monomer composites (**1**⊃BBMN and **1**⊃BBMA). The monomers were exclusively adsorbed inside the nanochannels, as confirmed by X-ray powder diffraction (XRPD), thermogravimetric (TG) and N$_2$ adsorption measurements (Supplementary Figs. 4–6). Polymerization of BBMN and BBMA was then conducted by heating the composites at 250 °C (below the temperature of monomer release from the pores) for 24 h in a sealed glass tube, resulting in the composites of **1** with poly(naphthalene-2,3:6,7-tetrayl-6,7-dimethylene) (PNTD) and poly(anthracene-2,3:6,7-tetrayl-6,7-dimethylene) (PATD), respectively. We confirmed the formation of the composites (**1**⊃PNTD and **1**⊃PATD) using a series of characterization techniques. XRPD measurements showed that the crystal structure of the host MOF was maintained during the heating process (Supplementary Fig. 4). The morphology and size of the particles of **1** remained unchanged during the polymerization, as confirmed by scanning electron microscopy (Supplementary Fig. 7). These results suggest that polymerization proceeded inside the channels of **1**. Furthermore, a drastic decrease in the N$_2$ adsorption capacity of the composites compared with that of the pristine **1** was consistent with the accommodation of the precursor polymers in the nanochannels (Supplementary Fig. 6).

The precursor polymers, PNTD and PATD, were released from the framework of **1** by digesting the host in an aqueous NaOH solution. The complete removal of **1** was confirmed by XRPD (Supplementary Fig. 4) and scanning electron microscopy–energy-dispersive X-ray spectroscopy (Supplementary Fig. 8). We performed structural characterizations of the products using Fourier transform infrared (FTIR), solid-state ^{13}C nuclear magnetic resonance (NMR) and matrix-assisted laser desorption/ionization time-of-flight mass spectroscopy (MALDI-TOF-MS) measurements. The FTIR spectra of PNTD and PATD display peaks corresponding to the out-of-plane (opla) sp^2 C–H vibration mode, which contrast with the product obtained from thermal processing the bulk monomers under the same conditions (Supplementary Figs. 2 and 9), suggesting inhibition of the cross-linking reaction in
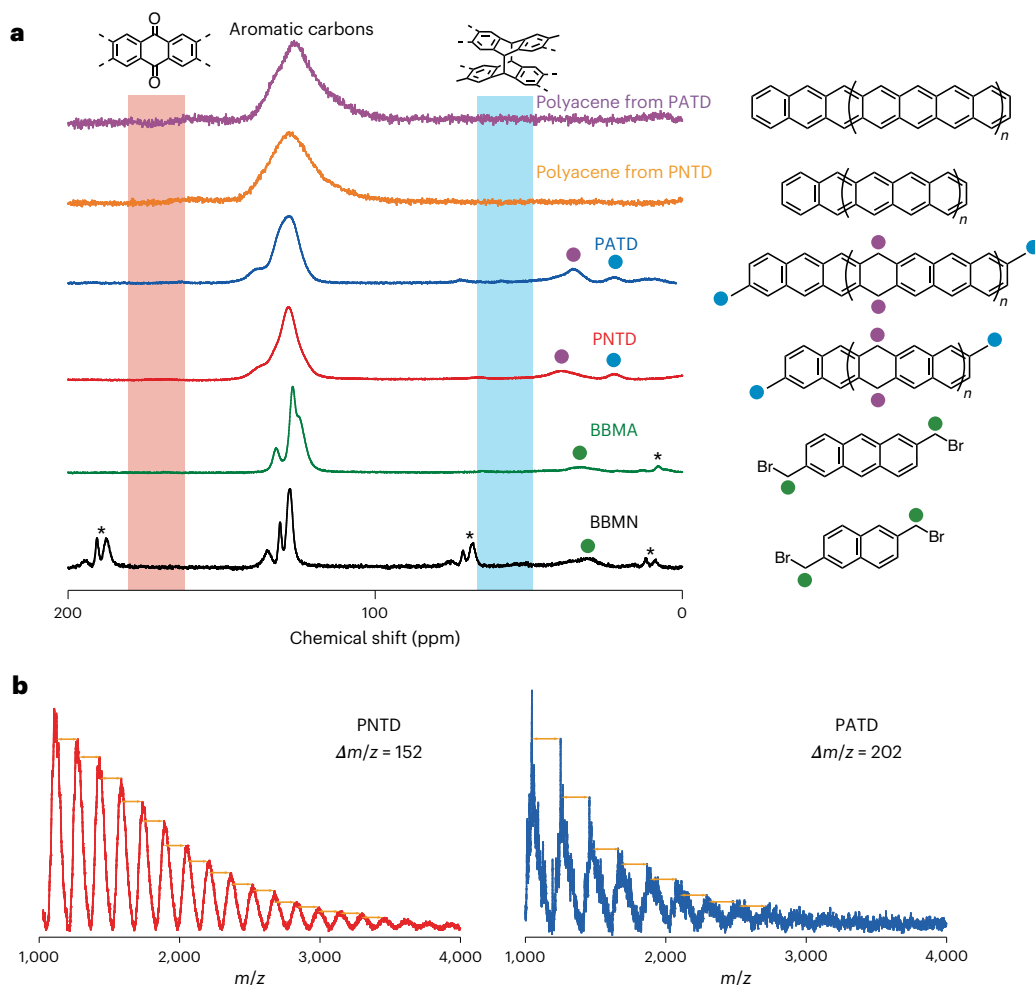
Fig. 2 | Synthesis of precursors and polyacene using an MOF. a, Solid-state ^{13}C NMR spectra of BBMN, BBMA, PNTD, PATD and polyacene. The coloured circles indicate the signals assigned to sp^3 carbons of the monomers and precursor polymers. The asterisk (*) corresponds to spinning side bands. **b**, MALDI-TOF-MS (linear mode) spectra of PNTD (red) and PATD (blue). The orange arrows represent the repeating mass interval of the precursor polymers.

the MOF channels. Notably, the ^{13}C NMR spectra represent the characteristic signals of the polymeric hydroacenes (Fig. 2a). Formation of the polymers resulted in a complete loss of the bromomethyl group; concomitantly, the appearance of resonance ascribable to the carbon of the methylene group was observed. Additionally, a cluster of peaks, assignable to aromatic carbons[35], was observed around 120–140 ppm. In the PNTD spectrum, the peak intensity for the aromatic carbons at the zigzag positions was higher than that of the BBMN heated without the MOF, supporting the progress of site-selective linear polymerization within the 1-D channels of **1** (Supplementary Fig. 10). The peak at 20 ppm was attributed to the methyl terminus of the polymers via the debromination reaction[36]. The absence of other peaks indicates that the precursor polymers did not undergo any undesired side reactions, such as oxidation and dimerization, during their isolation process. The formation of polymeric compounds was corroborated by the MALDI-TOF-MS spectra, which showed a periodic pattern of signals in agreement with the molecular mass of the repeating unit (Fig. 2b and Supplementary Fig. 11). Remarkably, the precursor polymers consisted of up to several dozens of linearly fused rings, demonstrating the generation of highly extended polymeric hydroacenes mediated by the MOF nanochannels.

The precursor polymers were transformed into polyacene with numerous benzene rings by heating at 300 °C under air atmosphere. The colour of the samples drastically changed from ochre to dark brown during the heating treatment, suggesting the formation of polyacene with an extended conjugated backbone. In contrast, the transformation

reaction did not proceed at all under vacuum conditions, demonstrating that oxygen is essential for the dehydro-aromatization reaction (Supplementary Fig. 12). The obtained polyacene was insoluble in all solvents due to the strong interchain π–π interaction, which may impede microscopic structural analysis; however, the bulk quantity of polyacene meant a wide range of techniques could be used to confirm the conversion of the precursors to polyacene. For instance, solid-state ^{13}C NMR spectroscopy of polyacene did not exhibit the signals for terminal methyl groups of the precursor polymers, presumably because of thermally induced elimination (Fig. 2a). Most strikingly, the methylene resonance peak completely disappeared. The presence of only a broad peak in the aromatic region confirms the formation of polyacene via quantitative dehydro-aromatization reaction[7,37]. This is also confirmed by the presence of characteristic polyacene peaks in FTIR spectroscopy measurements. The *opla* aromatic C–H vibration modes are classified as SOLO, DUO, TRIO and QUATRO, in reference to the number of adjacent C–H groups[38]. Only the SOLO and QUATRO mode were detected at 900 and 736 cm^{-1}, respectively, as was the case with the unsubstituted acene series (Fig. 3a)[39,40]. The disappearance of the DUO-mode band at approximately 800 cm^{-1} suggests the removal of the terminal methyl groups in the precursor polymers during the heating process[38,39,41], which is consistent with NMR analysis (Fig. 2a).

We attempted to analyse the polyacene chain length using MALDI-TOF-MS measurements; however, no mass peak corresponding to polyacene was detectable, probably because of its high molecular weight
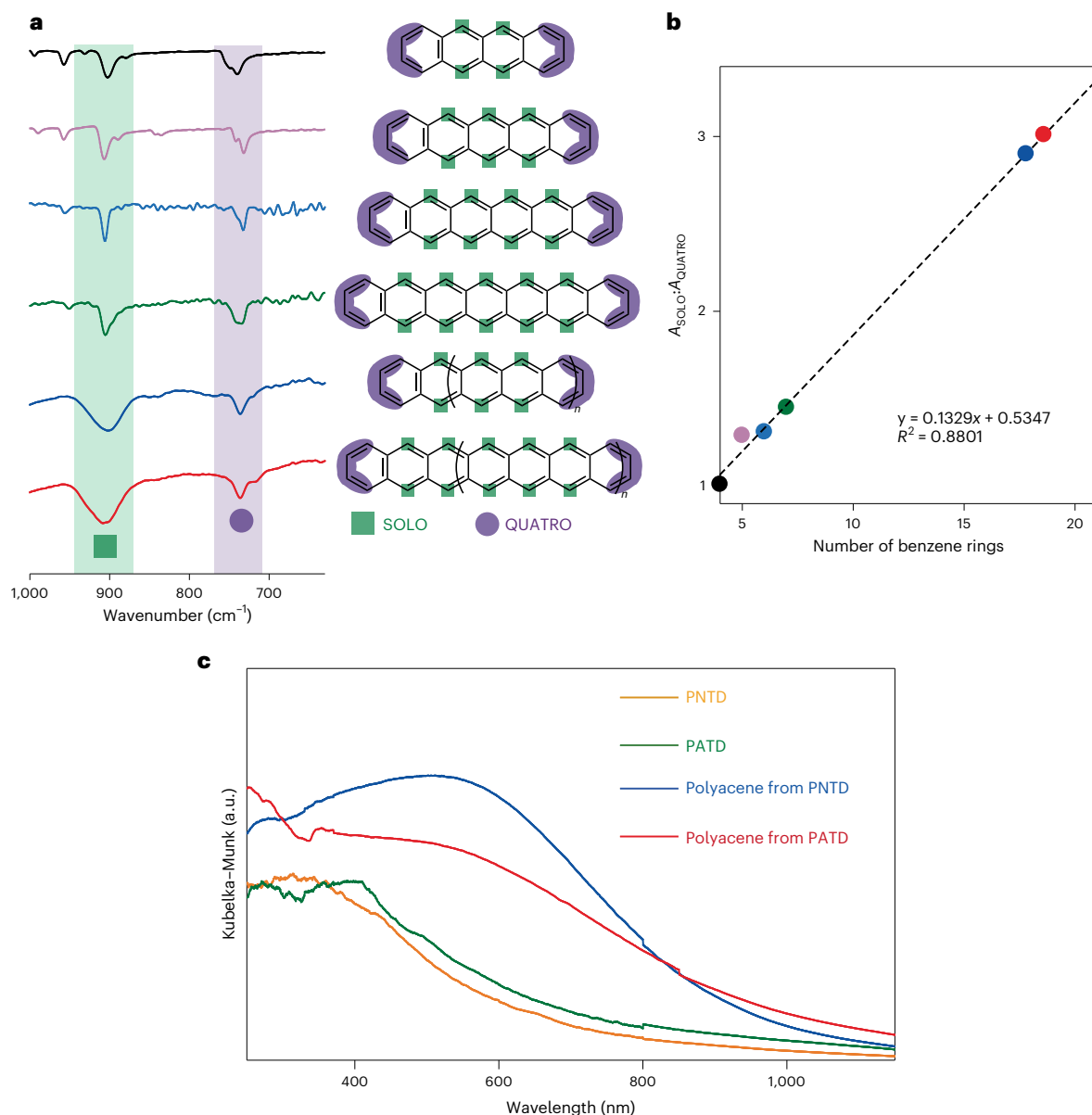
Fig. 3 | Analysis of polyacene structure. a, FTIR spectra of tetracene, pentacene, hexacene, heptacene and polyacene synthesized from PNTD and PATD. **b**, The relative peak area of SOLO to QUATRO vibration modes (A_{SOLO}:A_{QUATRO}) plotted against benzene ring number for the acene series. (black, tetracene; purple, pentacene; sky blue, hexacene; green, heptacene; blue, polyacene from PNTD; red, polyacene from PATD). The mean number of benzene rings in polyacene was evaluated using the correlation between A_{SOLO}:A_{QUATRO} and the number of benzene rings (dotted line). **c**, Solid-state UV–visible light–near-IR absorption spectra of PNTD, PATD and polyacene. Polyacene is the mixture of extended acenes with a different chain length, giving rise to broad absorption over a wide wavelength, ranging from visible light to near IR, which is in contrast to the previously reported acene series[7,44].

and strong intermolecular interactions which reduced the detection efficiency of polyacene. Therefore, because vibrational spectroscopy is a powerful method for quantitative structural analysis, we analysed polyacene length using IR[42,43]. The peaks corresponding to the *opla sp²* C–H vibration modes (SOLO and QUATRO) of the previously reported acene series were analysed and we found a correlation between those peaks and the number of the benzene rings, demonstrating that the IR analysis is capable of evaluating polyacene length (Supplementary Fig. 13)[39]. Therefore, several acene molecules with defined structures were synthesized and simulated for IR analysis (Fig. 3 and Supplementary Fig. 14), revealing a linear correlation between the relative peak area of SOLO to QUATRO modes and the benzene ring number. According to the line of best fit, the mean numbers (±S.D.) of benzene rings in polyacene from PNTD and PATD were estimated to be 17.8 ± 3.3 and 18.6 ± 3.5, respectively (Fig. 3b). Additionally, the absorption spectra

of polyacene corroborated the presence of acenes with numerous fused benzene rings. The S_0 to S_1 transition band of acenes (*p* band) shifts bathochromically with increasing size of the acene system[44,45]. The polyacene exhibited substantial absorption bands in the near-IR region (Fig. 3c). The bandgaps of polyacene from PNTD and PATD were estimated to be 1.30 and 1.28 eV, respectively, on the basis of the absorbance onsets, which were notably small enough to be comparable with the theoretical limit value (1.23 eV) for acenes with infinite chain length[44]. Also, given that the precursor polymers consisted of up to several dozen rings (Fig. 2b and Supplementary Fig. 11), these results indicate that, to our knowledge, the polyacene obtained in this study is the longest among the acene series reported so far.

The unprecedented length of the generated polyacene incentivized our efforts to unveil its physicochemical properties. The study on the structural stability of polyacene produced remarkable results.
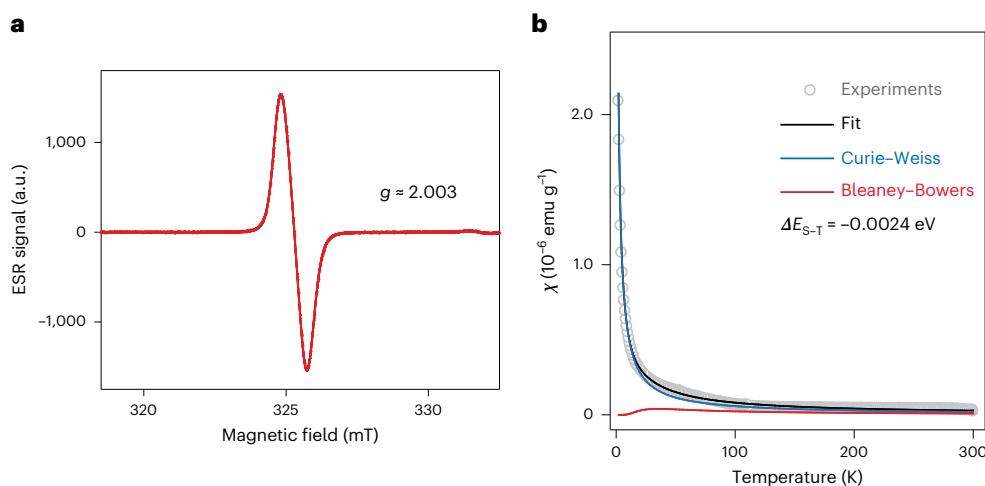
a

b

Fig. 4 | Magnetic properties of polyacene. a, ESR spectrum of polyacene synthesized from PATD. No hyperfine splitting was observed, suggesting the delocalization of spin density along the polymer chains. **b**, Temperature dependence of the magnetic susceptibility χ (grey circle) of polyacene prepared from PATD. The magnetic susceptibility plots could be fitted to the sum (black line) of Curie–Weiss (blue line) and Bleaney–Bowers (red line) equations. The singlet–triplet energy gap (ΔE_{S-T}) of polyacene was calculated to be −0.0024 eV by the Bleaney–Bowers equation, which is smaller than the theoretical value for polyacene with infinite chain length[50], probably due to the intermolecular spin–spin interaction in the bulk state[51].

It is well known that longer acenes are more susceptible to oxidation and dimerization reactions because of their inherent singlet biradical character[46,47]. However, the ^{13}C NMR spectra of polyacene did not show the peaks for sp^3-bridgehead carbons[37] and carbonyl groups generated by these reactions (Fig. 2a). Therefore, we concluded that such unfavourable reactions did not take place in the bulk polyacene; therefore, we evaluated the biradical character of polyacene using electron spin resonance (ESR) and superconducting quantum interfering device (SQUID). In the ESR spectrum of polyacene, we observed a signal with a g value of 2.003, ascribable to a carbon-centred radical (Fig. 4a and Supplementary Fig. 15a)[48]. SQUID polyacene data revealed a fitting component with a steep decrease in the magnetic susceptibility upon cooling from 70 to 20 K, in accordance with the Bleaney–Bowers equation (Supplementary Fig. 15b)[49]. This magnetic behaviour is typical for open-shell singlet biradical molecules[50]; therefore, these results suggested that polyacene did have a biradical nature, which is in agreement with theoretical calculations[51–53]. This is also supported by the NMR polyacene analysis: we detected NMR signals that were broader than those of the precursors which were ascribed to a thermally populated paramagnetic triplet biradical (Fig. 2a)[48].

To identify the mechanisms underlying the unexpectedly high stability of polyacene, the biradical species were quantitatively analysed by ESR. The spin concentration of polyacene was calculated to be approximately 1×10^{18} spins g^{-1} (Fig. 4a). Notably, this value is several orders of magnitude smaller than that predicted from the length of polyacene[54]. A similar reduction in radical nature has been reported for several π-conjugated radical molecules that form π-dimers in the solid state. The intermolecular antiferromagnetic interactions result in these molecules being undetectable via ESR[55]. The insolubility of polyacene in all solvents implied strong interchain interactions; therefore, the aggregation of polyacene was studied using MD simulations, and the π-stacked structure was energetically most stable (Supplementary Fig. 16a). The aggregation structure was also revealed by XRPD of the polyacene sample, showing a peak corresponding to π–π stacking (Supplementary Fig. 16b). The observed broad diffraction peak suggested the presence of the stacked structures with non-uniform interchain distance, as shown in the MD structure of polyacene. Therefore, it is probable that interchain antiferromagnetic coupling occurs when in close proximity, giving rise to the decrease in the inherent biradical character of polyacene[56,57].

We evaluated the composition of polyacene using X-ray photoelectron spectroscopy by initially focusing on the surface of the polyacene particles. The C_{1s} core level region displays peaks corresponding to the oxidized carbon (Supplementary Fig. 17). The surface of the polyacene particles was etched using argon plasma to examine the inner composition, which led to a drastic decrease in the oxidized carbon peaks. We observed a small NMR peak, assignable to the oxidized carbons (Supplementary Fig. 18), when polyacene was left in air for a long period (>30 days). These results suggest that the oxidation reaction took place only near the surface of the polyacene particles owing to their biradical character. The high stability of the bulk polyacene was also confirmed by TG analysis, which showed no weight loss up to 350 °C (Supplementary Fig. 19a). The FTIR spectra of polyacene before and after heating up to 350 °C displayed no obvious changes, and the *opla* sp^2 C–H vibration modes were clearly observable, indicating its high thermal stability (Supplementary Fig. 19b). Again, this behaviour was in sharp contrast to that of acenes in solution, which readily decompose via oxidation and/or dimerization reactions. Therefore, the unexpectedly high stability of polyacene in the solid state can be attributed to the chain aggregation that decreased its biradical character, limited oxygen access to the polymer chains and restricted the chain motion required for undesirable oxidation and dimerization reactions[7,11,37,39,58,59].

Conclusions

Unsubstituted acenes have thus far been fabricated on surfaces under ultrahigh vacuum conditions because of their unstable zigzag edges[15,60], presenting a barrier to their scalability. Here, we used an MOF to demonstrate the bulk-scale synthesis of polyacenes with exceptional length. The physicochemical properties of the acene series depending on benzene ring number led to the development of theoretical arguments[45,61,62]. Our findings represent an important step toward not only unveiling the unique topological properties of the acene series[63,64] but also its future applications in various areas, including molecular electronics, optoelectronics and spintronics. For example, polyacene, being a mixture of polymeric chains with different lengths, is capable of absorbing light over a wide wavelength, ranging from visible to near IR (Fig. 3c). Along with its remarkably high stability, this light-absorbing feature would be beneficial for applications in photoenergy conversion systems.

Methods

Synthesis of precursor polymers in 1

The general procedure for synthesis was as follows: Degassed 1 was prepared by heating it at 160 °C for 12 h in a vacuum. BBMN (298 mg) and degassed 1 (1,000 mg) were mixed in a round-bottom flask (20 ml) and heated at 150 °C for 1 h under reduced pressure, leading to vapour adsorption of BBMN throughout the internal and external surface of 1. The externally absorbed monomer was selectively removed by heating at 150 °C for 12 h under vacuum, affording a composite of 1 including BBMN (1⊃BBMN, 1,237 mg). The amount of BBMN adsorbed in the composite was calculated to be 18.7%, as determined by TG measurements. 1⊃BBMN was then heated at 250 °C in a sealed reaction container for 24 h to perform polymerization, resulting in 1 and PNTD nanocomposite (1⊃PNTD, 1,124 mg). PATD was synthesized identically within the nanochannels from BBMA (loading amount of BBMA was 33.5%).

Isolation of precursor polymers from 1

1⊃PNTD (1,680 mg) was stirred in a 1 M aqueous solution of NaOH (120 ml) for 24 h, followed by washing three times with a 5% v/v aqueous solution of HF (20 ml) for complete decomposition of the host framework. The collected PNTD was washed with $CHCl_3$ and then dried under reduced pressure to obtain PNTD (123 mg, 70% yield based on the loading amount of BBMN in 1⊃BBMN). PATD was isolated from 1 in a similar manner (39% yield).

Conversion from PNTD and PATD to polyacene

The precursor polymers, PNTD (48 mg) and PATD (24 mg), were heated at 300 °C under air for 24 h to obtain polyacene of 38 and 18 mg, respectively.

Reporting summary

Further information on research design is available in the Nature Portfolio Reporting Summary linked to this article.

Data availability

The data supporting the findings of this study are available within the article and its Supplementary Information. Source data are provided with this paper.

References

1. Mills, W. H. & Mills, M. CCXXX.—The synthetical production of derivatives of dinaphthanthracene. *J. Chem. Soc. Trans.* **101**, 2194–2208 (1912).
2. Congreve, D. N. et al. External quantum efficiency above 100% in a singlet-exciton-fission-based organic photovoltaic cell. *Science* **340**, 334–337 (2013).
3. Anthony, J. E. Functionalized acenes and heteroacenes for organic electronics. *Chem. Rev.* **106**, 5028–5048 (2006).
4. Lee, D. et al. In vivo imaging of hydrogen peroxide with chemiluminescent nanoparticles. *Nat. Mater.* **6**, 765–769 (2007).
5. Tateishi, K. et al. Room temperature hyperpolarization of nuclear spins in bulk. *Proc. Natl Acad. Sci. USA* **111**, 7527–7530 (2014).
6. Tönshoff, C. & Bettinger, H. F. Pushing the limits of acene chemistry: the recent surge of large acenes. *Chem. Eur. J.* **27**, 3193–3212 (2021).
7. Watanabe, M. et al. The synthesis, crystal structure and charge-transport properties of hexacene. *Nat. Chem.* **4**, 574–578 (2012).
8. Yue, W., Suraru, S.-L., Bialas, D., Müller, M. & Würthner, F. Synthesis and properties of a new class of fully conjugated azahexacene analogues. *Angew. Chem. Int. Ed.* **53**, 6159–6162 (2014).
9. Liang, Z., Tang, Q., Xu, J. & Miao, Q. Soluble and stable N-heteropentacenes with high field-effect mobility. *Adv. Mater.* **23**, 1535–1539 (2011).
10. Clar, E. *Polycyclic Hydrocarbons* (Academic Press, 1964).
11. Müller, M., Ahrens, L., Brosius, V., Freudenberg, J. & Bunz, U. H. F. Unusual stabilization of larger acenes and heteroacenes. *J. Mater. Chem. C* **7**, 14011–14034 (2019).
12. Kaur, I., Jazdzyk, M., Stein, N. N., Prusevich, P. & Miller, G. P. Design, synthesis, and characterization of a persistent nonacene derivative. *J. Am. Chem. Soc.* **132**, 1261–1263 (2010).
13. Urgel, J. I. et al. On-surface light-induced generation of higher acenes and elucidation of their open-shell character. *Nat. Commun.* **10**, 861 (2019).
14. Krüger, J. et al. Tetracene formation by on-surface reduction. *ACS Nano.* **10**, 4538–4542 (2016).
15. Eisenhut, F. et al. Dodecacene generated on surface: reopening of the energy gap. *ACS Nano.* **14**, 1011–1017 (2020).
16. Schmidt, B. V. K. J. Metal-organic frameworks in polymer science: polymerization catalysis, polymerization environment, and hybrid materials. *Macromol. Rapid Commun.* **41**, 1900333 (2020).
17. Kitao, T., Zhang, Y., Kitagawa, S., Wang, B. & Uemura, T. Hybridization of MOFs and polymers. *Chem. Soc. Rev.* **46**, 3108–3133 (2017).
18. Ding, N. et al. Partitioning MOF-5 into confined and hydrophobic compartments for carbon capture under humid conditions. *J. Am. Chem. Soc.* **138**, 10100–10103 (2016).
19. Distefano, G., Comotti, A., Bracco, S., Beretta, M. & Sozzani, P. Porous dipeptide crystals as polymerization nanoreactors. *Angew. Chem. Int. Ed.* **51**, 9258–9262 (2012).
20. Comotti, A. et al. Confined polymerization in highly ordered mesoporous organosilicas. *Chem. Eur. J.* **21**, 18209–18217 (2015).
21. Wu, C. G. & Bein, T. Conducting carbon wires in ordered, nanometer-sized channels. *Science* **266**, 1013–1015 (1994).
22. Lee, H. C. et al. Toward ultimate control of radical polymerization: functionalized metal–organic frameworks as a robust environment for metal-catalyzed polymerizations. *Chem. Mater.* **30**, 2983–2994 (2018).
23. Uemura, T., Ono, Y., Kitagawa, K. & Kitagawa, S. Radical polymerization of vinyl monomers in porous coordination polymers: nanochannel size effects on reactivity, molecular weight, and stereostructure. *Macromolecules* **41**, 87–94 (2008).
24. MacLean, M. W. A. et al. Unraveling inter- and intrachain electronics in polythiophene assemblies mediated by coordination nanospaces. *Angew. Chem. Int. Ed.* **55**, 708–713 (2016).
25. Mulzer, C. R. et al. Superior charge storage and power density of a conducting polymer-modified covalent organic framework. *ACS Cent. Sci.* **2**, 667–673 (2016).
26. Furukawa, H., Cordova, K. E., O'Keeffe, M. & Yaghi, O. M. The chemistry and applications of metal-organic frameworks. *Science* **341**, 2130444 (2013).
27. Kitagawa, S., Kitaura, R. & Noro, S. Functional porous coordination polymers. *Angew. Chem. Int. Ed.* **43**, 2334–2375 (2004).
28. Horcajada, P. et al. Porous metal-organic-framework nanoscale carriers as a potential platform for drug delivery and imaging. *Nat. Mater.* **9**, 172–178 (2010).
29. Sumida, K. et al. Carbon dioxide capture in metal-organic frameworks. *Chem. Rev.* **112**, 724–781 (2012).
30. Lee, J. et al. Metal-organic framework materials as catalysts. *Chem. Soc. Rev.* **38**, 1450–1459 (2009).
31. Kitaura, R. et al. Formation of a one-dimensional array of oxygen in a microporous metal-organic solid. *Science* **298**, 2358–2361 (2002).
32. Talin, A. A. et al. Tunable electrical conductivity in metal-organic framework thin-film devices. *Science* **343**, 66–69 (2014).
33. Zuzak, R. et al. Higher acenes by on-surface dehydrogenation: from heptacene to undecacene. *Angew. Chem. Int. Ed.* **57**, 10500–10505 (2018).
34. Guillerm, V. et al. A series of isoreticular, highly stable, porous zirconium oxide based metal-organic frameworks. *Angew. Chem. Int. Ed.* **51**, 9267–9271 (2012).

35. Dorel, R., McGonigal, P. R. & Echavarren, A. M. Hydroacenes made easy by gold(I) catalysis. *Angew. Chem. Int. Ed.* **55**, 11120–11123 (2016).

36. Guan, B. T. et al. Methylation of arenes via Ni-catalyzed aryl C–O/F activation. *Chem. Commun. (Camb.)* **(12)**, 1437–1439 (2008).

37. Einholz, R. et al. Heptacene: characterization in solution, in the solid state, and in films. *J. Am. Chem. Soc.* **139**, 4435–4442 (2017).

38. Centrone, A. et al. Structure of new carbonaceous materials: the role of vibrational spectroscopy. *Carbon* **43**, 1593–1609 (2005).

39. Jančařík, A. et al. Preparative-scale synthesis of nonacene. *Nat. Commun.* **13**, 223 (2022).

40. Mondal, R. et al. Synthesis, stability, and photochemistry of pentacene, hexacene, and heptacene: a matrix isolation study. *J. Am. Chem. Soc.* **131**, 14281–14289 (2009).

41. Yamada, Y. et al. Carbon materials with zigzag and armchair edges. *ACS Appl. Mater. Interfaces* **10**, 40710–40739 (2018).

42. Țucureanu, V., Matei, A. & Avram, A. M. FTIR spectroscopy for carbon family study. *Crit. Rev. Anal. Chem.* **46**, 502–520 (2016).

43. Sasaki, T., Yamada, Y. & Sato, S. Quantitative analysis of zigzag and armchair edges on carbon materials with and without pentagons using infrared spectroscopy. *Anal. Chem.* **90**, 10724–10731 (2018).

44. Shen, B., Tatchen, J., Sanchez-Garcia, E. & Bettinger, H. F. Evolution of the optical gap in the acene series: undecacene. *Angew. Chem. Int. Ed.* **57**, 10506–10509 (2018).

45. Korytár, R. et al. Signature of the Dirac cone in the properties of linear oligoacenes. *Nat. Commun.* **5**, 5000 (2014).

46. Bendikov, M. et al. Oligoacenes: theoretical prediction of open-shell singlet diradical ground states. *J. Am. Chem. Soc.* **126**, 7416–7417 (2004).

47. Zade, S. S. & Bendikov, M. Reactivity of acenes: mechanisms and dependence on acene length. *J. Phys. Org. Chem.* **25**, 452–461 (2012).

48. Huang, R. et al. Higher order π-conjugated polycyclic hydrocarbons with open-shell singlet ground state: nonazethrene versus nonacene. *J. Am. Chem. Soc.* **138**, 10323–10330 (2016).

49. Bleaney, B. & Bowers, K. D. Anomalous paramagnetism of copper acetate. *Proc. R. Soc. A* **214**, 451–465 (1952).

50. Dressler, J. J. et al. Thiophene and its sulfur inhibit indenoindenodibenzothiophene diradicals from low-energy lying thermal triplets. *Nat. Chem.* **10**, 1134–1140 (2018).

51. Hachmann, J., Dorando, J. J., Aviles, M. & Chan, G. K. L. The radical character of the acenes: a density matrix renormalization group study. *J. Chem. Phys.* **127**, 134309 (2007).

52. Qu, Z., Zhang, D., Liu, C. & Jiang, Y. Open-shell ground state of polyacenes: a valence bond study. *J. Phys. Chem. A* **113**, 7909–7914 (2009).

53. Barker, J. E. et al. Molecule isomerism modulates the diradical properties of stable singlet diradicaloids. *J. Am. Chem. Soc.* **142**, 1548–1555 (2020).

54. Trinquier, G., David, G. & Malrieu, J. P. Qualitative views on the polyradical character of long acenes. *J. Phys. Chem. A* **122**, 6926–6933 (2018).

55. Fukui, K. et al. Electronic structure of a stable phenalenyl radical in crystalline state as studied by SQUID measurements, cw-ESR, and ^{13}C CP/MAS NMR spectroscopy. *Synth. Met.* **103**, 2257–2258 (1999).

56. Xiang, Q. et al. Stable olympicenyl radicals and their π-dimers. *J. Am. Chem. Soc.* **142**, 11022–11031 (2020).

57. Sato, H. et al. Drastic effect of water-adsorption on the magnetism of carbon nanomagnets. *Solid State Commun.* **125**, 641–645 (2003).

58. Miura, T., Kitao, T. & Uemura, T. Nanoconfinement of an otherwise useless fluorophore in metal–organic frameworks to elicit and tune emission. *J. Phys. Chem. C* **126**, 6628–6636 (2022).

59. Hayashi, H. et al. Visible-light-induced heptacene generation under ambient conditions: utilization of single-crystal interior as an isolated reaction site. *Chem. Eur. J.* **26**, 15079–15083 (2020).

60. Mishra, S. et al. Large magnetic exchange coupling in rhombus-shaped nanographenes with zigzag periphery. *Nat. Chem.* **13**, 581–586 (2021).

61. Schmitteckert, P., Thomale, R., Korytár, R. & Evers, F. Incommensurate quantum-size oscillations in acene-based molecular wires—effects of quantum fluctuations. *J. Chem. Phys.* **146**, 092320 (2017).

62. Miao, Y. et al. Mechanism of length-induced magnetism in polyacene molecules. *Phys. Rev. B* **105**, 094419 (2022).

63. Karakonstantakis, G., Liu, L., Thomale, R. & Kivelson, S. A. Correlations and renormalization of the electron-phonon coupling in the honeycomb Hubbard ladder and superconductivity in polyacene. *Phys. Rev. B* **88**, 224512 (2013).

64. Ulbricht, R. et al. Carrier dynamics in semiconductors studied with time-resolved terahertz spectroscopy. *Rev. Mod. Phys.* **83**, 543–586 (2011).

Author contributions

T.U. conceived of and directed the project. T.K. and T.M. designed and performed the experiments. T.U. codesigned the experiments. Y.T. and S.S. contributed to ESR measurements. R.N. and T.H. assisted with SQUID measurements. Y.S.C., H.H. and H.Y. synthesized the precursor molecules of hexacene and heptacene. T.K., T.M. and T.U. wrote the manuscript, with input from all the co-authors.

Competing interests

The authors declare no competing interests.

Additional information

Supplementary information The online version contains supplementary material available at https://doi.org/10.1038/s44160-023-00310-w.

Correspondence and requests for materials should be addressed to Takashi Uemura.

Peer review information *Nature Synthesis* thanks Dan Zhao and the other, anonymous, reviewer(s) for their contribution to the peer review of this work. Primary Handling Editor: Alison Stoddart, in collaboration with the *Nature Synthesis* team.

Reprints and permissions information is available at www.nature.com/reprints.

Publisher's note Springer Nature remains neutral with regard to jurisdictional claims in published maps and institutional affiliations.

nature portfolio

Corresponding author(s): Takahi Uemura

Last updated by author(s): Mar 17, 2023

Reporting Summary

Nature Portfolio wishes to improve the reproducibility of the work that we publish. This form provides structure for consistency and transparency in reporting. For further information on Nature Portfolio policies, see our Editorial Policies and the Editorial Policy Checklist.

Statistics

For all statistical analyses, confirm that the following items are present in the figure legend, table legend, main text, or Methods section.

n/a	Confirmed	
☐	☒	The exact sample size (*n*) for each experimental group/condition, given as a discrete number and unit of measurement
☐	☒	A statement on whether measurements were taken from distinct samples or whether the same sample was measured repeatedly
☒	☐	The statistical test(s) used AND whether they are one- or two-sided *Only common tests should be described solely by name; describe more complex techniques in the Methods section.*
☒	☐	A description of all covariates tested
☒	☐	A description of any assumptions or corrections, such as tests of normality and adjustment for multiple comparisons
☒	☐	A full description of the statistical parameters including central tendency (e.g. means) or other basic estimates (e.g. regression coefficient) AND variation (e.g. standard deviation) or associated estimates of uncertainty (e.g. confidence intervals)
☒	☐	For null hypothesis testing, the test statistic (e.g. *F*, *t*, *r*) with confidence intervals, effect sizes, degrees of freedom and *P* value noted *Give P values as exact values whenever suitable.*
☒	☐	For Bayesian analysis, information on the choice of priors and Markov chain Monte Carlo settings
☒	☐	For hierarchical and complex designs, identification of the appropriate level for tests and full reporting of outcomes
☒	☐	Estimates of effect sizes (e.g. Cohen's *d*, Pearson's *r*), indicating how they were calculated

Our web collection on statistics for biologists contains articles on many of the points above.

Software and code

Policy information about availability of computer code

Data collection	Molecular dynamics simulation and density functional theory calculation were performed using Materials Studio (version 8.0; Accelrys, San Diego, CA).
Data analysis	*Provide a description of all commercial, open source and custom code used to analyse the data in this study, specifying the version used OR state that no software was used.*

For manuscripts utilizing custom algorithms or software that are central to the research but not yet described in published literature, software must be made available to editors and reviewers. We strongly encourage code deposition in a community repository (e.g. GitHub). See the Nature Portfolio guidelines for submitting code & software for further information.

Data

Policy information about availability of data

All manuscripts must include a data availability statement. This statement should provide the following information, where applicable:

- Accession codes, unique identifiers, or web links for publicly available datasets
- A description of any restrictions on data availability
- For clinical datasets or third party data, please ensure that the statement adheres to our policy

The data supporting the findings of this study are available within the Article and its Supplementary Information.

Human research participants

Reporting on sex and gender	*Use the terms sex (biological attribute) and gender (shaped by social and cultural circumstances) carefully in order to avoid confusing both terms. Indicate if findings apply to only one sex or gender; describe whether sex and gender were considered in study design whether sex and/or gender was determined based on self-reporting or assigned and methods used. Provide in the source data disaggregated sex and gender data where this information has been collected, and consent has been obtained for sharing of individual-level data; provide overall numbers in this Reporting Summary. Please state if this information has not been collected. Report sex- and gender-based analyses where performed, justify reasons for lack of sex- and gender-based analysis.*
Population characteristics	*Describe the covariate-relevant population characteristics of the human research participants (e.g. age, genotypic information, past and current diagnosis and treatment categories). If you filled out the behavioural & social sciences study design questions and have nothing to add here, write "See above."*
Recruitment	*Describe how participants were recruited. Outline any potential self-selection bias or other biases that may be present and how these are likely to impact results.*
Ethics oversight	*Identify the organization(s) that approved the study protocol.*

Note that full information on the approval of the study protocol must also be provided in the manuscript.

Field-specific reporting

Please select the one below that is the best fit for your research. If you are not sure, read the appropriate sections before making your selection.

☐ Life sciences   ☐ Behavioural & social sciences   ☐ Ecological, evolutionary & environmental sciences

For a reference copy of the document with all sections, see nature.com/documents/nr-reporting-summary-flat.pdf

Life sciences study design

All studies must disclose on these points even when the disclosure is negative.

Sample size	*Describe how sample size was determined, detailing any statistical methods used to predetermine sample size OR if no sample-size calculation was performed, describe how sample sizes were chosen and provide a rationale for why these sample sizes are sufficient.*
Data exclusions	*Describe any data exclusions. If no data were excluded from the analyses, state so OR if data were excluded, describe the exclusions and the rationale behind them, indicating whether exclusion criteria were pre-established.*
Replication	*Describe the measures taken to verify the reproducibility of the experimental findings. If all attempts at replication were successful, confirm this OR if there are any findings that were not replicated or cannot be reproduced, note this and describe why.*
Randomization	*Describe how samples/organisms/participants were allocated into experimental groups. If allocation was not random, describe how covariates were controlled OR if this is not relevant to your study, explain why.*
Blinding	*Describe whether the investigators were blinded to group allocation during data collection and/or analysis. If blinding was not possible, describe why OR explain why blinding was not relevant to your study.*

Behavioural & social sciences study design

All studies must disclose on these points even when the disclosure is negative.

Study description	*Briefly describe the study type including whether data are quantitative, qualitative, or mixed-methods (e.g. qualitative cross-sectional, quantitative experimental, mixed-methods case study).*
Research sample	*State the research sample (e.g. Harvard university undergraduates, villagers in rural India) and provide relevant demographic information (e.g. age, sex) and indicate whether the sample is representative. Provide a rationale for the study sample chosen. For studies involving existing datasets, please describe the dataset and source.*
Sampling strategy	*Describe the sampling procedure (e.g. random, snowball, stratified, convenience). Describe the statistical methods that were used to predetermine sample size OR if no sample-size calculation was performed, describe how sample sizes were chosen and provide a rationale for why these sample sizes are sufficient. For qualitative data, please indicate whether data saturation was considered, and what criteria were used to decide that no further sampling was needed.*

Data collection	Provide details about the data collection procedure, including the instruments or devices used to record the data (e.g. pen and paper, computer, eye tracker, video or audio equipment) whether anyone was present besides the participant(s) and the researcher, and whether the researcher was blind to experimental condition and/or the study hypothesis during data collection.
Timing	Indicate the start and stop dates of data collection. If there is a gap between collection periods, state the dates for each sample cohort.
Data exclusions	If no data were excluded from the analyses, state so OR if data were excluded, provide the exact number of exclusions and the rationale behind them, indicating whether exclusion criteria were pre-established.
Non-participation	State how many participants dropped out/declined participation and the reason(s) given OR provide response rate OR state that no participants dropped out/declined participation.
Randomization	If participants were not allocated into experimental groups, state so OR describe how participants were allocated to groups, and if allocation was not random, describe how covariates were controlled.

Ecological, evolutionary & environmental sciences study design

All studies must disclose on these points even when the disclosure is negative.

Study description	Briefly describe the study. For quantitative data include treatment factors and interactions, design structure (e.g. factorial, nested, hierarchical), nature and number of experimental units and replicates.
Research sample	Describe the research sample (e.g. a group of tagged Passer domesticus, all Stenocereus thurberi within Organ Pipe Cactus National Monument), and provide a rationale for the sample choice. When relevant, describe the organism taxa, source, sex, age range and any manipulations. State what population the sample is meant to represent when applicable. For studies involving existing datasets, describe the data and its source.
Sampling strategy	Note the sampling procedure. Describe the statistical methods that were used to predetermine sample size OR if no sample-size calculation was performed, describe how sample sizes were chosen and provide a rationale for why these sample sizes are sufficient.
Data collection	Describe the data collection procedure, including who recorded the data and how.
Timing and spatial scale	Indicate the start and stop dates of data collection, noting the frequency and periodicity of sampling and providing a rationale for these choices. If there is a gap between collection periods, state the dates for each sample cohort. Specify the spatial scale from which the data are taken
Data exclusions	If no data were excluded from the analyses, state so OR if data were excluded, describe the exclusions and the rationale behind them, indicating whether exclusion criteria were pre-established.
Reproducibility	Describe the measures taken to verify the reproducibility of experimental findings. For each experiment, note whether any attempts to repeat the experiment failed OR state that all attempts to repeat the experiment were successful.
Randomization	Describe how samples/organisms/participants were allocated into groups. If allocation was not random, describe how covariates were controlled. If this is not relevant to your study, explain why.
Blinding	Describe the extent of blinding used during data acquisition and analysis. If blinding was not possible, describe why OR explain why blinding was not relevant to your study.

Did the study involve field work? ☐ Yes ☐ No

Field work, collection and transport

Field conditions	Describe the study conditions for field work, providing relevant parameters (e.g. temperature, rainfall).
Location	State the location of the sampling or experiment, providing relevant parameters (e.g. latitude and longitude, elevation, water depth).
Access & import/export	Describe the efforts you have made to access habitats and to collect and import/export your samples in a responsible manner and in compliance with local, national and international laws, noting any permits that were obtained (give the name of the issuing authority, the date of issue, and any identifying information).
Disturbance	Describe any disturbance caused by the study and how it was minimized.

Reporting for specific materials, systems and methods

We require information from authors about some types of materials, experimental systems and methods used in many studies. Here, indicate whether each material, system or method listed is relevant to your study. If you are not sure if a list item applies to your research, read the appropriate section before selecting a response.

Materials & experimental systems			Methods		
n/a	**Involved in the study**		**n/a**	**Involved in the study**	
☒	☐ Antibodies		☒	☐ ChIP-seq	
☒	☐ Eukaryotic cell lines		☒	☐ Flow cytometry	
☒	☐ Palaeontology and archaeology		☒	☐ MRI-based neuroimaging	
☒	☐ Animals and other organisms				
☒	☐ Clinical data				
☒	☐ Dual use research of concern				